

Competing Germene and Germylene Extrusion from Photolysis of 1,1-Diarylgermacyclobutanes. Substituent Effects on Germene Reactivity

William J. Leigh,* Gregory D. Potter, Lawrence A. Huck, and Adroha Bhattacharya

Department of Chemistry, McMaster University, 1280 Main Street West,
Hamilton, Ontario, Canada L8S 4M1

Received June 22, 2008

Direct irradiation of 1,1-diphenyl-, 1,1-bis[4-(trifluoromethyl)phenyl]-, and 1,1-bis[3,5-bis(trifluoromethyl)phenyl]germacyclobutanes (**2**, **4**, and **5**, respectively) in methanolic C₆D₁₂ solution affords products consistent with the competing formation of the corresponding 1,1-diarylgermenes and diarylgermylenes, along with ethylene and cyclopropane. The relative yields of the two Ge-containing primary products (germene:germylene) vary with the extent of CF₃ substitution on the aryl rings, decreasing in the order **2** > **4** > **5**. As was reported previously for **2**, laser flash photolysis of **4** and **5** in hexane, acetonitrile, or tetrahydrofuran solution allows the detection of the corresponding transient 1,1-diarylgermenes (**6** and **7**, respectively), which have been identified on the basis of their UV/vis spectra ($\lambda_{\text{max}} \sim 325$ nm) and quenching studies with MeOH, *tert*-butyl alcohol (*t*-BuOH), acetic acid (AcOH), *n*-butylamine (*n*-BuNH₂), and acetone. In carefully dried hexane solution, weak transient absorptions assignable to the corresponding germynes and their respective (digermene) dimers are also observed; in the case of **5**, these assignments have been confirmed by the results of steady-state and laser photolysis experiments with 1,1-bis[3,5-bis(trifluoromethyl)phenyl]-2,3-dimethyl-1-germacyclopent-3-ene (**14c**), which affords the germylene exclusively, in a substantially higher quantum yield. The reactivities of the germenes toward each of the various substrates studied vary modestly with aryl substituent, increasing in the order acetone < *t*-BuOH < MeOH \approx *n*-BuNH₂ < AcOH. The rate constants increase with increasing trifluoromethyl substitution in the cases of alcohol and acetone addition but decrease correspondingly in the case of AcOH addition. Substrate acidity thus plays a much more dominant role in the reactions of the Ge=C bond with nucleophilic reagents than is the case with the homologous silene derivatives, whose reaction kinetics are controlled primarily by substrate nucleophilicity.

Introduction

There has been great interest in the chemistry of homo- and heteronuclear heavier group 14 ethylene analogues, focusing principally on the synthesis and structural characterization of derivatives stabilized kinetically with sterically bulky substituents.^{1–8} Much less attention has been paid to the study of simpler derivatives that are typically transient species in fluid solution, whose direct detection and study typically require the use of fast time-resolved spectroscopic methods and a photochemical reaction for the formation of the transient species of interest. While a significant body of experimental data now exists on the kinetics and mechanisms of the reactions of transient silenes and disilenes in

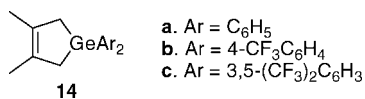
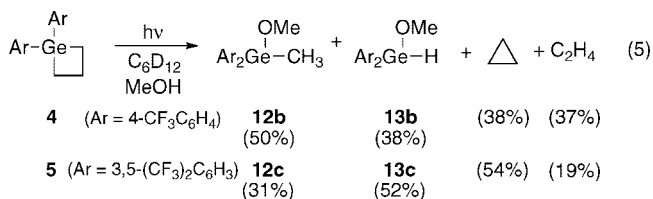
solution,^{9–16} relatively little has been done with their organogermanium counterparts, germenes and digermenes.^{17–19}

Some time ago, we published the results of a study of the prototypical 1,1-diarylgermene derivative, 1,1-diphenylgermene (**1**), by steady-state and laser flash photolysis methods, employing the UV photolysis of 1,1-diphenylgermacyclobutane (**2**; eq 1) to generate this highly reactive molecule in solution.¹⁷ Its spectroscopic properties and reactivity toward aliphatic alcohols and acetic acid were studied in various

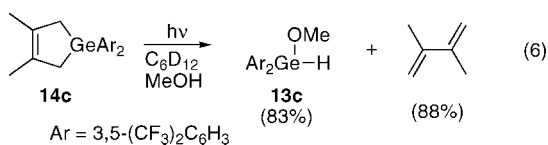
(1) Wiberg, N. *J. Organomet. Chem.* **1984**, 273, 141.
(2) Baines, K. M.; Stibbs, W. G. *Adv. Organomet. Chem.* **1996**, 39, 275.
(3) Driess, M.; Grützmacher, H. *Angew. Chem., Int. Ed. Engl.* **1996**, 35, 828.
(4) Escudie, J.; Couret, C.; Ranaivonjatovo, H. *Coord. Chem. Rev.* **1998**, 180, 565.
(5) Escudie, J.; Ranaivonjatovo, H. *Adv. Organomet. Chem.* **1999**, 44, 113.
(6) Power, P. P. *Chem. Rev.* **1999**, 99, 3463.
(7) Tokitoh, N.; Okazaki, R. *Adv. Organomet. Chem.* **2001**, 47, 121.
(8) Tokitoh, N.; Okazaki, R.; Rappoport, Z. In *The Chemistry of Organic Germanium, Tin and Lead Compounds*; Rappoport, Z., Ed.; Wiley: New York, 2002; Vol. 2, Part 1, pp 843–901.

(9) Morkin, T. L.; Owens, T. R.; Leigh, W. J.; Rappoport, Z.; Apeloig, Y. In *The Chemistry of Organic Silicon Compounds*; Rappoport, Z., Ed.; Wiley: New York, 2001; Vol. 3, pp 949–1026.

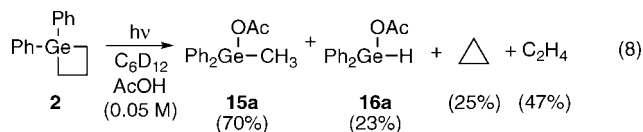
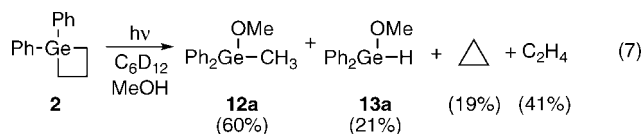
(10) Leigh, W. J.; Li, X. *Organometallics* **2002**, 21, 1197.
(11) Leigh, W. J.; Li, X. *J. Phys. Chem. A* **2003**, 107, 1517.
(12) Owens, T. R.; Harrington, C. R.; Pace, T. C. S.; Leigh, W. J. *Organometallics* **2003**, 22, 5518.
(13) Samuel, M. S.; Jenkins, H. A.; Hughes, D. W.; Baines, K. M. *Organometallics* **2003**, 22, 1603.
(14) Owens, T. R.; Grinyer, J.; Leigh, W. J. *Organometallics* **2005**, 24, 2307.
(15) Leigh, W. J.; Owens, T. R.; Bendikov, M.; Zade, S. S.; Apeloig, Y. *J. Am. Chem. Soc.* **2006**, 128, 10772.
(16) Milnes, K. K.; Baines, K. M. *Organometallics* **2007**, 26, 2392.
(17) Toltl, N. P.; Leigh, W. J. *J. Am. Chem. Soc.* **1998**, 120, 1172.
(18) Leigh, W. J. *Pure Appl. Chem.* **1999**, 71, 453.
(19) Huck, L. A.; Leigh, W. J. *Organometallics* **2007**, 26, 1339.
(20) Leigh, W. J.; Bradaric, C. J.; Kerst, C.; Banisch, J. H. *Organometallics* **1996**, 15, 2246.
(21) Leigh, W. J.; Sluggett, G. W. *J. Am. Chem. Soc.* **1994**, 116, 10468.
(22) Nagase, S.; Kudo, T. *Organometallics* **1984**, 3, 324.
(23) Bradaric, C. J.; Leigh, W. J. *Organometallics* **1998**, 17, 645.



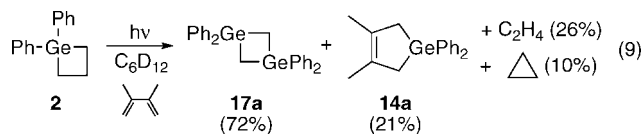
under similar conditions. Compound **14c** was prepared and its photochemistry studied in the course of the present work. Photolysis of the compound in methanolic C₆D₁₂ was found to afford **13c** and 2,3-dimethyl-1,3-butadiene (DMB) in chemical yields of 83% and 88%, respectively, as established by concentration vs time plots over the 0–20% conversion range in **14c** (eq 6). The quantum yield for formation of **13c** from this compound was determined to be $\Phi_{13c} = 0.45 \pm 0.09$, again using the photolysis of **14a** under the same conditions as the actinometer (Figure S3, Supporting Information).



The observation of significant yields of **13b,c** in the photo-product mixtures from **4** and **5** prompted us to re-examine the photochemistry of the parent compound (**2**) under similar conditions, as the corresponding product (diphenylmethoxygermane, **13a**) was not detected as a photoproduct in our original study of **2**.¹⁷ Indeed, ¹H NMR analysis of a photolyzed 0.041 M solution of **2** in C₆D₁₂ containing 0.3 M MeOH revealed that both **12a** and **13a** are formed as products, in chemical yields of ca. 60% and 21%, respectively, along with ethylene and cyclopropane (eq 7 and Figure S2 in the Supporting Information). Analogous results were obtained using acetic acid (AcOH; 0.05 M) as trapping agent, which (at low conversions) cleanly afforded the acetoxygermanes **15a** and **16a** in yields of ca. 70% and 25%, respectively (eq 8 and Figure S4 in the Supporting Information). Our failure to detect the germylene-derived products (**13a** and **16a**) in our earlier study is not really understood but could be due to the fact that the original experiments were carried out using dichloromethane as an internal NMR integration standard, which may have facilitated decomposition of the compounds during photolysis due to some radical chain process. On the other hand, it is clear that cyclopropane was formed in our original study of **2**, as a minor photoproduct characterized in the ¹H NMR spectra by a singlet at δ 0.20 (in C₆D₁₂); unfortunately, however, we did not pursue its identification. The quantum yields for the formation of **12a** and **13a** from the photolysis of **2** were also determined (using the photolysis of **14a** under the same conditions as actinometer; $\Phi_{13a} = 0.55 \pm 0.07^{24}$) and found to be $\Phi_{12a} = 0.17 \pm 0.04$ and $\Phi_{13a} = 0.060 \pm 0.015$. The results are in good agreement with the quantum yield for photolysis of **2** reported in our original study ($\Phi_{-2a} = 0.24 \pm 0.04$).¹⁷



Photolysis of a 0.05 M solution of **2** in C₆D₁₂ containing DMB (0.04 M) led to the formation of digermacyclobutane **17a** and germacyclopentene **14a** in yields of 72% and 21%, respectively, along with ethylene and cyclopropane (see eq 9); the use of a deficiency of the diene in the experiment was predicated by its higher extinction coefficient at 254 nm compared to that of **2**. The two Ge-containing products were identified by comparison of their ¹H NMR and mass spectral data to those of authentic samples; their yields relative to consumed **2** were determined from the slopes of concentration vs time plots, determined from ¹H NMR spectra of the reaction mixture recorded throughout the photolysis. While the formation of one or more additional (minor) unidentified products was evident in the ¹H NMR spectrum of the photolyzed mixture (see Figure S5 in the Supporting Information), no evidence for the formation of the seemingly most likely candidate(s)—a cycloadduct between the diene and germene **1**—could be obtained by GC/MS analysis of the crude photolysate. In any event, the fact that the head-to-tail dimer **17a** remains the major germene-derived product in the presence of 0.04 M DMB indicates that the diene is a relatively inefficient trapping agent for transient germenes, in contrast to its well-known effectiveness as a germylene scavenger.^{8,25}



Compounds **4** and **5** were also photolyzed in deoxygenated C₆D₁₂ containing acetone (0.2 M), with the mixtures being monitored by ¹H NMR spectroscopy. The resulting spectra after ca. 50% conversion were quite complex in both cases and showed broad baseline absorptions in the aromatic and δ 0.5–2 regions of the spectra, suggestive of the formation of polymeric material. Ethylene and cyclopropane were the only products that could be conclusively identified in the two photolysates, and no resonances other than that due to ethylene could be detected in the vinylic region of the spectra in either case.

The results of the steady-state photolysis experiments with **2**, **4**, and **5** under various conditions show that the photochemistry of these compounds is characterized by two competing reaction channels, one leading to the formation of the corresponding 1,1-diarylgermene and ethylene by formal (2+2) cycloreversion and one leading to the corresponding diarylgermylene and cyclopropane by formal (1+3) cycloreversion (eq 10). The efficiency of product formation from **2** is unaffected by added DMB, which is expected to be a good triplet quencher for compounds of this type. From this it can be concluded that both reaction pathways result from the excited singlet states of the germacyclobutanes. Most interestingly, the partitioning between the (2+2) and (1+3) cycloreversion pathways varies with the extent of trifluoromethyl substitution, from ca. 3:1 in favor of the (2+2) pathway in the case of the parent compound **2** to ca. 1:2 in favor of the (1+3) pathway in the case of the bis[3,5-bis(trifluoromethyl)phenyl] derivative **5**. It should be

(25) Neumann, W. P.; Weisbeck, M. P.; Wienken, S. *Main Group Met. Chem.* **1994**, *17*, 151.

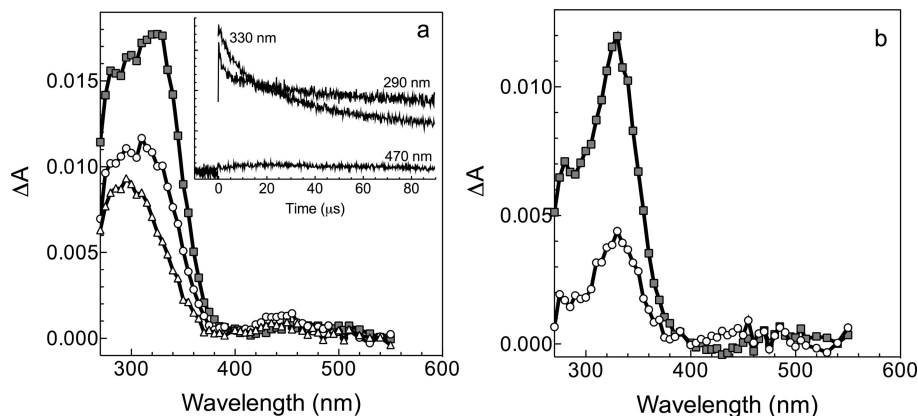


Figure 1. (a) Transient absorption spectra recorded 0–0.32 μs (■), 20.2–20.5 μs (○), and 88.3–88.6 μs (△) after the laser pulse, by laser flash photolysis of a 0.4 mM solution of **4** in deoxygenated hexane at 25 °C. The inset shows transient decay traces recorded at 290, 330, and 470 nm under the two sets of conditions. (b) Difference spectra calculated from the spectra of Figure 1a: (■) (0–0.32 μs) – (88.3–88.6 μs); (○) (20.2–20.5 μs) – (88.3–88.6 μs).

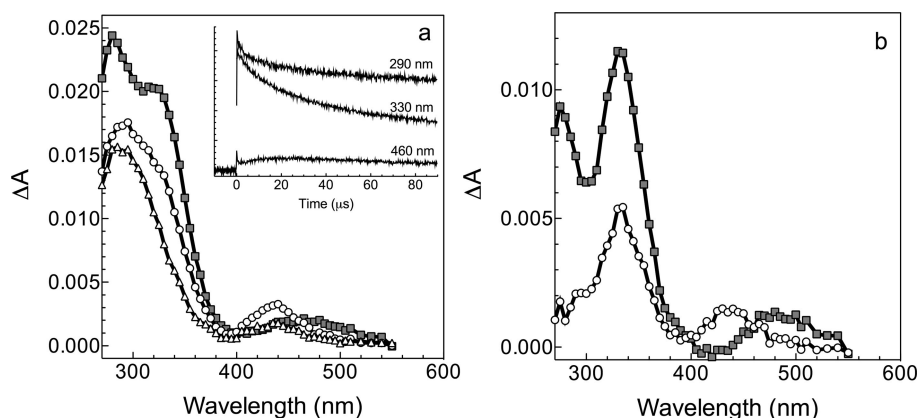
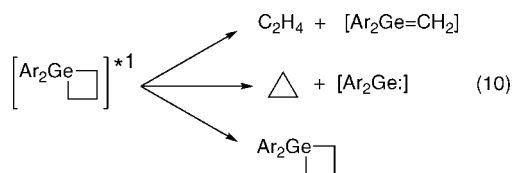


Figure 2. (a) Transient absorption spectra recorded (■) 0–0.32 μs , (○) 20.2–20.5 μs , and (△) 88.3–88.6 μs after the laser pulse, by laser flash photolysis of a 0.6 mM solution of **5** in deoxygenated hexane at 25 °C. The inset shows transient decay traces recorded at 290, 330, and 460 nm under the two sets of conditions. (b) Difference spectra calculated from the spectra of Figure 2a: (■) (0–0.32 μs) – (88.3–88.6 μs); (○) (20.2–20.5 μs) – (88.3–88.6 μs).

noted that propene could not be detected as a coproduct in any of the three cases, indicating that cyclopropane is the exclusive organic product of the (1+3) photocycloreversion process. In contrast, the thermal (gas phase) decomposition of 1,1-dimethylgermacyclobutane is known to afford ethylene and both cyclopropane and propene, along with products derived from 1,1-dimethylgermene and dimethylgermylene.²⁶ In the thermal reaction, however, the formation of the two C_3H_6 hydrocarbons was proposed to result from fundamentally different reaction pathways.²⁶



Laser Flash Photolysis Studies. Laser flash photolysis experiments were carried out using a KrF excimer laser for excitation (248 nm, ~25 ns, 100 mJ) and a thermostated flow system for sample delivery. Flash photolysis of deoxygenated solutions of **4** (ca. 0.53 mM) and **5** (ca. 0.70 mM) in dry hexane afforded strong transient absorptions centered in the 280–340

nm range, along with much weaker transient absorptions in the 400–520 nm region of the spectra. For example, Figure 1a shows transient UV/vis spectra recorded with **4** in deoxygenated hexane over three selected time windows after the laser pulse; analogous data for **5** under similar conditions are shown in Figure 2a. In both cases, a relatively strong transient absorption centered at $\lambda_{\text{max}} \sim 330$ nm with lifetime $\tau \sim 20$ μs is produced with the laser pulse, superimposed on a second, much longer lived absorption that is centered at shorter wavelengths and has a lifetime of a few milliseconds or greater. The presence of O_2 had little to no effect on the intensities or lifetimes of the 330 nm transients but reduced the intensities of both the long-lived absorptions and the weak absorptions above 400 nm; these effects were more pronounced in O_2 -saturated solution than in air-saturated solution; examples of transient spectra recorded for **4** and **5** in air-saturated hexane are included in the Supporting Information (Figure S6). Addition of 1 mM AcOH led to a distinct shortening of the lifetimes of the 330 nm transients and eliminated the others entirely; this was also observed in the presence of MeOH, *tert*-butyl alcohol (*t*-BuOH), and acetone (vide infra). The spectra and lifetimes of the 330 nm species are similar to those reported previously for 1,1-diphenylgermene (**1**) under similar conditions ($\tau \sim 20$ μs ; $\lambda_{\text{max}} 325$ nm),¹⁷ and we thus assign them to the 1,1-diarylgermenes **6** and **7**, respectively; the sensitivity of their lifetimes to nucleophilic

(26) Namavari, M.; Conlin, R. T. *Organometallics* **1992**, *11*, 3307.

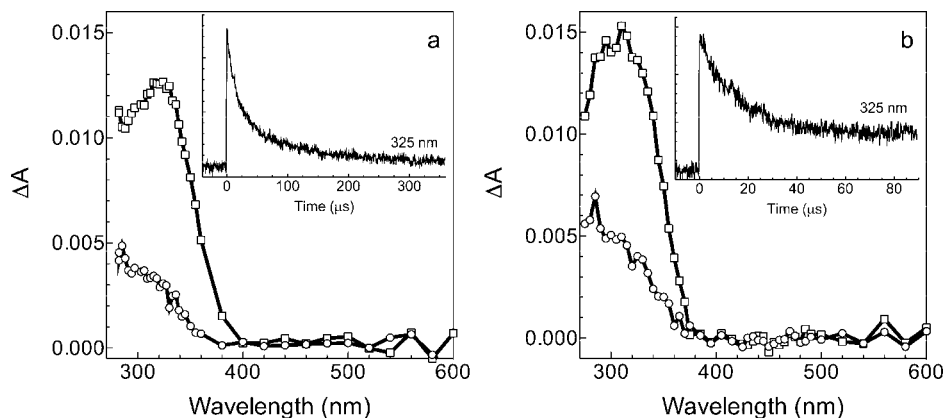
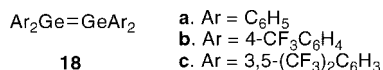


Figure 3. Transient absorption spectra recorded (□) 0.1–0.6 μ s and (○) 62.1–62.7 μ s after the laser pulse, by laser flash photolysis of deoxygenated MeCN solutions of (a) **4** (0.5 mM) and (b) **5** (0.7 mM). The insets show decay traces recorded at 325 nm.

reagents and the lack of sensitivity to oxygen are also consistent with the germene assignments. The identities of the long-lived species absorbing below 300 nm are unknown, but the fact that they are eliminated in the presence of substrates that are reactive toward germenes and/or germynes suggests they are secondary products formed by reaction of the primary transient photoproducts.

The weak transient absorptions arising in the 400–520 nm spectral range were significantly stronger from **5** than from **4** and exhibited temporal behavior that was very different from those of the shorter wavelength absorptions. In both cases, evidence for two distinct transient species with overlapping absorption spectra was clearly discernible, one species with λ_{max} centered at 480–500 nm that was formed with the laser pulse and decayed relatively rapidly ($0.2 < \tau < 2 \mu$ s), and a second centered at λ_{max} 440 nm that grew in after the laser pulse and then decayed over several hundred microseconds with mixed-order kinetics. Neither species could be detected at all unless adequate care was taken to dry the solvent and sample delivery system. We assign the promptly formed species to the germynes **8** and **9** and the 440 nm species to their dimerization products, tetraaryldigermenes **18b,c**, on the basis of the similarity of the spectra and temporal behavior to those observed using the 1,1-diarylgermacyclopent-3-enes **14b**¹⁹ and **14c** (vide infra) as precursors to **8** and **9**, respectively, and the fact that their formation is quenched upon addition of nucleophilic substrates that are known to react rapidly with **8** and other related transient diarylgermylenes.^{19,27,28} The relative weakness of the signals observed for **8** and **9** in flash photolysis experiments with **4** and **5** is undoubtedly due to the rather low quantum yields for their formation from these compounds, coupled with the low extinction coefficients that characterize the UV/vis absorption spectra of diarylgermylenes.^{24,29,30}



Figures 1b and 2b show difference spectra, calculated by subtracting the 88.3–88.6 μ s spectra of Figures 1a and 2a, respectively, from those recorded immediately and 20.2–20.5 μ s after laser excitation of **4** and **5**. The two sets of spectra thus isolate those components of the transient spectra that decay during the first 90 μ s after the (ca. 20 ns) laser pulse. In both cases, the end-of-pulse difference spectrum can be seen to

consist of the sum of the spectra of the corresponding germene (λ_{max} 330 nm) and germylene (λ_{max} 280, 480–500 nm); it should be noted that, as would be expected on the basis of the product studies, the intensity of the germylene absorptions relative to that of the germene is much higher from **5** than from **4**, consistent with a higher relative yield of germylene from photolysis of the former compound. Comparison of the first and second difference spectra shows that, in both cases, the germenes decay to roughly half their initial concentrations within ca. 20 μ s, while the germylene absorptions at 280 and 480–500 nm are replaced by the longer lived absorptions due to the corresponding digermenes (λ_{max} 440 nm).

Spectra recorded in deoxygenated acetonitrile (MeCN) and tetrahydrofuran (THF) solution showed transient absorptions similar to those observed in hexane solution in the region below 360 nm, but they were devoid of any detectable transient absorptions in the 400–600 nm range of the spectrum (see Figure 3), due presumably to rapid reaction (or complexation) of the germynes (**8** and **9**) with the solvent (vide infra). Both sets of spectra consisted of two overlapping transient absorptions in MeCN solution, one centered at $\lambda_{\text{max}} \sim 325$ nm with lifetime $\tau \sim 15 \mu$ s and a second with $\lambda_{\text{max}} < 300$ nm and $\tau \geq 100 \mu$ s. As in the experiments in hexane solution, the contribution from the longer lived species was significantly reduced in air-saturated solution, while the lifetimes and intensities of the 325 nm absorptions were largely unaffected. Addition of alcohols or acetic acid to the solutions shortened the lifetimes of the 325 nm species (vide infra), consistent with their assignment to germenes **6** and **7**. Transient spectra recorded by flash photolysis of **4** in deoxygenated tetrahydrofuran (THF) solution were much cleaner than those in hexane or MeCN, showing a single transient species exhibiting $\lambda_{\text{max}} \sim 325$ nm and lifetime $\tau \sim 4 \mu$ s. A quenching experiment with MeOH (vide infra) confirmed the identity of the species as germene **6**. There was no change in the position or breadth of the absorption, or the transient lifetime, upon lowering the temperature of the solution to ca. 4 °C. Thus, we could obtain no evidence for Lewis acid–base complexation between the germene and the O-donor solvent over the 4–25 °C temperature range.

The germylene (**9**) and digermene (**18c**) assignments in the laser photolysis experiments with **5** in hexane were confirmed by laser photolysis of 1.3 mM hexane solutions of germacyclo-

(27) Leigh, W. J.; Harrington, C. R. *J. Am. Chem. Soc.* **2005**, *127*, 5084.

(28) Leigh, W. J.; Lollmahomed, F.; Harrington, C. R.; McDonald, J. M. *Organometallics* **2006**, *25*, 5424.

(29) Tokitoh, N.; Kishikawa, K.; Okazaki, R.; Sasamori, T.; Nakata, N.; Takeda, N. *Polyhedron* **2003**, *21*, 563.

(30) Kira, M.; Ishida, S.; Iwamoto, T.; Ichinohe, M.; Kabuto, C.; Ignatovich, L.; Sakurai, H. *Chem. Lett.* **1999**, *1999*, 263.

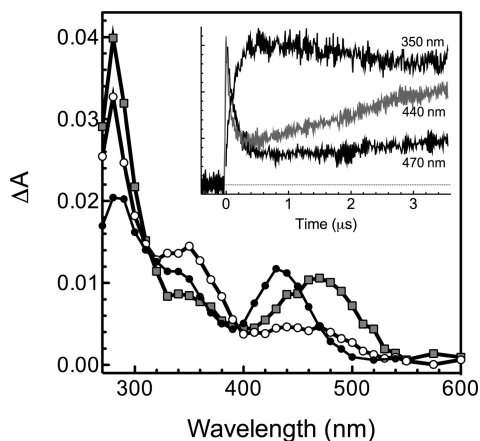
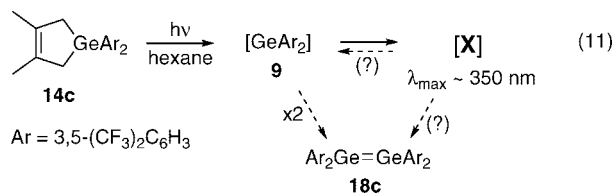


Figure 4. Transient absorption spectra recorded (■) 58–70 ns, (○) 0.32–0.34 μs , and (●) 9.6–9.9 μs after the laser pulse, by laser flash photolysis of a 3 mM solution of 1,1-diaryl-3,4-dimethylgermacyclopent-3-ene **14c** in dry, deoxygenated hexane at 25 °C. The inset shows transient absorption vs time profiles recorded at 470, 440, and 350 nm.

pent-3-ene **14c**. This compound afforded results consistent with the sequential formation of *three* distinct transient species, as illustrated in Figure 4. The first species is formed within the laser pulse and exhibits $\lambda_{\text{max}} \sim 475$ nm and lifetime $\tau \sim 200$ ns and the second species ($\lambda_{\text{max}} \sim 350$ nm; $\tau \sim 10$ μs) is formed concomitantly with the decay of the first-formed species, while the third species ($\lambda_{\text{max}} \sim 440$ nm; $\tau > 200$ μs) is formed on a time scale similar to that of the decay of the second-formed species. On the basis of our previous results for other related 1,1-diarylgermacyclopent-3-ene derivatives (e.g., **14a,b**),^{19,24} we assign the first and third species to germylene **9** and digermene **18c**, respectively; their temporal behavior was quite similar to what was observed at 475 and 440 nm, respectively, in the experiments with **5** in hexane (vide supra). A conclusive assignment cannot be made at the present time for the intermediate (second-formed) species, which could not be detected in the experiments with **5** because of overlap with the strong absorptions due to germene **7** in this region. We initially suspected that the species might be a complex formed by reaction of germylene **9** with adventitious water or other oxygenated impurities in the solvent, as both its spectrum and its temporal characteristics (as well as the temporal characteristics of the other two species detected) are similar to what we have observed previously for diarylgermylenes in hexane containing small amounts of THF or aliphatic alcohols.^{19,28} However, flash photolysis experiments with solutions of **14c** in a sample of hexane distilled from LiAlH_4 afforded results very similar to those described above, which employed alumina-dried hexane. A second possibility is that the species is a complex formed by interaction of **9** with the C=C bond or fluorine atoms³¹ in its precursor (**14c**); however, experiments carried out with a more dilute (0.5 mM) solution of **14c** afforded weaker signals, as expected, but transient temporal behavior very similar to that observed with the higher precursor concentration. Whatever its identity, the results indicate that the formation of this species coincides with the decay of the free germylene, and the species somehow mediates the formation of digermene **18c**, either as a direct intermediate or as a nonreactive spectator in equilibrium with the free germylene (see eq 11). Establishing its identity is the subject of future work.



Further support for the germylene and digermene assignments in the flash photolysis experiments with **14c** was obtained upon addition of acetic acid (AcOH) to the solution, which caused the lifetime of the prompt (germylene) absorption to be shortened and the intensities of the signals centered at 350 and 440 nm to be reduced and eventually eliminated, all in proportion to the concentration of added substrate. Transient decays recorded at 500 nm in the presence of 0.2–0.8 mM AcOH decayed cleanly to the baseline with pseudo-first-order kinetics, and a plot of the first-order decay rate constant (k_{decay}) vs [AcOH] was linear, affording a quenching rate coefficient of $k_{\text{AcOH}} = (7.0 \pm 0.6) \times 10^9 \text{ M}^{-1} \text{ s}^{-1}$ (see eq 12). The value is in line with what would be expected on the basis of the reported rate constants for quenching of other substituted diarylgermylenes by AcOH in this solvent, which established a value of $k_{\text{AcOH}} = (6.2 \pm 1.0) \times 10^9 \text{ M}^{-1} \text{ s}^{-1}$ for germylene **8** and a Hammett ρ value of $\rho \approx +0.2$.¹⁹ The lifetime of the 440 nm absorption (assigned to digermene **18c**) is also shortened in the presence of the carboxylic acid; a plot of estimated k_{decay} values vs [AcOH] over the 0.1–0.8 mM concentration range in which the species remained detectable afforded a value of $k_{\text{AcOH}} = (2.2 \pm 0.8) \times 10^8 \text{ M}^{-1} \text{ s}^{-1}$ for the quenching rate constant. This too is consistent with previously published results for other transient tetraaryldigermenes.¹⁹

$$k_{\text{decay}} = k_0 + k_{\text{Q}}[\text{Q}] \quad (12)$$

Flash photolysis of deoxygenated solutions of **14b,c** in MeCN afforded strong, long-lived transient absorptions throughout the 280–380 nm range, which behaved similarly to one another but were completely unlike those observed with **4** and **5** under similar conditions; the two compounds exhibited prompt, long-lived absorptions centered at ca. 290 nm that decayed with complex kinetics over several milliseconds, along with shorter-lived absorptions centered in the 350–370 nm range that grew in over the first ca. 20 μs after the pulse and decayed to ca. 25% of their maximum intensities over ca. 200 μs . We include a representative set of data in the Supporting Information but defer a full interpretation of the results to a future publication. The main point of these experiments was to verify that the 325 nm species observed by flash photolysis of **4** and **5** in MeCN are unique to those compounds and are not due to species derived from reaction or complexation of the corresponding germylene coproducts with the nitrile solvent and can thus be most reasonably assigned to germenes **6** and **7**, respectively. The very pronounced differences in the spectra and temporal behavior of the transients observed from **14b/14c** and **4/5** in MeCN leave little doubt that the germene assignments are correct.

As mentioned above, addition of MeOH, *tert*-butyl alcohol (*t*-BuOH), or acetic acid (AcOH) to hexane solutions of **4** and **5** caused the decay of the absorptions due to germenes **6** and **7** to accelerate, consistent with reaction with the substrate in each case. Transient profiles recorded at 325 nm fit well to the sum of two first-order exponential decays, the fast component of which accelerated as the substrate concentration was increased while the lifetime of the slow component was unaffected; the intensity of the latter component also diminished with increasing

(31) (a) Bender, J. E. I.; Banaszak Holl, M. M.; Kampf, J. W. *Organometallics* **1997**, *16*, 2743. (b) Bender, J. E. I.; Banaszak Holl, M. M.; Mitchell, A.; Wells, N. J.; Kampf, J. W. *Organometallics* **1998**, *17*, 5166.

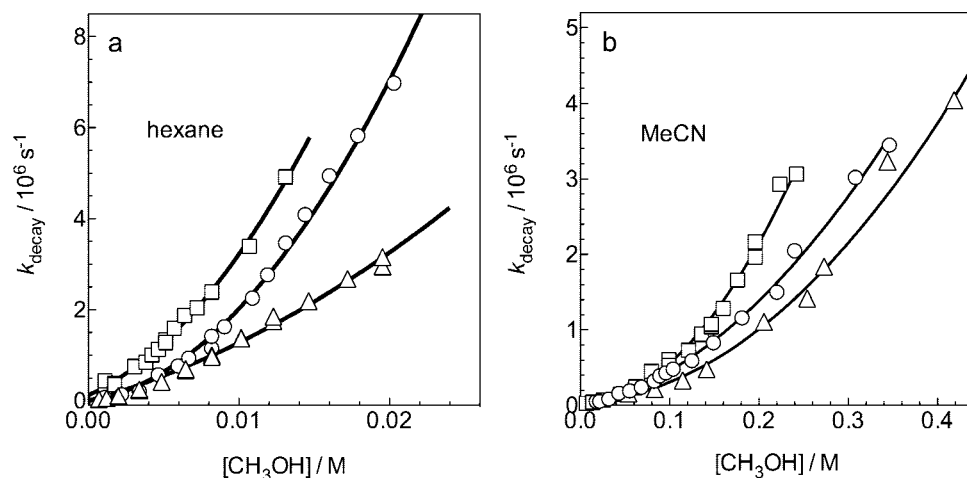


Figure 5. Plots of the pseudofirst order rate constants for germene decay (k_{decay}) for quenching of germenes (Δ) **1**, (\circ) **6**, and (\square) **7** versus $[\text{MeOH}]$ in (a) air-saturated hexane solution and (b) air-saturated MeCN solution at 25 °C. The solid lines are the best fits of the data to eq 13.

Table 1. Rate Constants for Reaction of Germenes **1**, **6**, and **7** and 1,1-Diphenylsilene (**3**) with Various Substrates in Hexane Solution at 25 °C (in Units of $10^7 \text{ M}^{-1} \text{ s}^{-1}$ or $10^7 \text{ M}^{-2} \text{ s}^{-1}$)

substrate	1	6	7	3
MeOH	$(9.3 \pm 2.8) + (350 \pm 140)[\text{MeOH}]$	$(8.4 \pm 3.0) + (830 \pm 180)[\text{MeOH}]$	$(14.8 \pm 0.5) + (1620 \pm 340)[\text{MeOH}]$	190 ± 20^d
<i>t</i> -BuOH	$(2 \pm 1) + (12 \pm 9)[t\text{-BuOH}]^a$	$(2.1 \pm 0.2) + (96 \pm 4)[t\text{-BuOH}]$	$(4.3 \pm 1.9) + (160 \pm 40)[t\text{-BuOH}]$	40 ± 7^d
AcOH	490 ± 100^b	400 ± 90^b	370 ± 80^b	310 ± 30^d
<i>n</i> -BuNH ₂	5 ± 1^c	13.2 ± 0.3	$(18 \pm 2) + (4500 \pm 2000)[n\text{-BuNH}_2]$	649 ± 12^e
acetone	$<0.02^a$	0.081 ± 0.003	0.162 ± 0.005	38 ± 2^f

^a From ref 17. ^b The limiting ($[\text{AcOH}]_{\text{bulk}} \rightarrow 0$) slopes of plots of k_{decay} vs $[\text{AcOH}]_{\text{bulk}}$. ^c From ref 18. ^d From ref 20. ^e From ref 11. ^f From ref 23, in isooctane solution.

substrate concentration. Plots of k_{decay} for the fast-decaying component vs substrate (“Q”) concentration exhibited positive curvature for the two alcohols; examples are shown in Figure 5a for the quenching of **6** and **7** by MeOH. For comparison, Figure 5a also shows the results of a similar experiment with germacyclobutane **2**, which was repeated as part of the present work. The latter data are considerably more detailed than those published previously for this system but are consistent with what we found in our earlier study.¹⁷

The data of Figure 5a were fit to the quadratic expression of eq 13, where k_{ROH} and $k_{2\text{ROH}}$ are the effective second- and third-order rate coefficients, respectively, for reaction of the three transient germenes with MeOH and *t*-BuOH in hexane solution. The results of these analyses are given in Table 1. Though the errors are large in several cases, the data clearly indicate that the reaction is dominated by the overall third-order (second order in MeOH) pathway, with the rate coefficients increasing very modestly with increasing electron-withdrawing power of the substituents on the aryl rings. The variation in the third-order rate coefficients with substituent is larger for *t*-BuOH, which is the less reactive of the two alcohols by a significant margin.

$$k_{\text{decay}} = k_0 + k_{\text{ROH}}[\text{ROH}] + k_{2\text{ROH}}[\text{ROH}]^2 \quad (13)$$

Plots of k_{decay} vs $[\text{AcOH}]$ exhibited *negative* curvature for both **6** and **7** over the 0–1 mM range in added carboxylic acid (see Figure S10 in the Supporting Information). Quenching of germene **1** by AcOH was investigated over the same concentration range and was found to exhibit similar characteristics. It should be noted that the rate constant reported in ref 17 for the reaction of **1** with AcOH in hexane was determined by linear analysis of a much more limited set of k_{decay} values that were recorded over the 1–3.5 mM concentration range in added AcOH and was thus underestimated quite significantly. The

Table 2. Rate Constants for Reaction of Germenes **1**, **6**, and **7** and 1,1-Diphenylsilene (**3**) with MeOH(D) and AcOH(D) in MeCN Solution at 25 °C

substrate	1	6	7
$k_{2\text{MeOH}}/10^7 \text{ M}^{-2} \text{ s}^{-1}$	2.3 ± 0.1	2.98 ± 0.07	5.3 ± 0.2
$k_{2\text{MeOD}}/10^7 \text{ M}^{-2} \text{ s}^{-1}$		2.15 ± 0.06	3.45 ± 0.09
$k_{\text{AcOH}}/10^7 \text{ M}^{-1} \text{ s}^{-1}$	64 ± 4	53 ± 2	46 ± 1
$k_{\text{AcOD}}/10^7 \text{ M}^{-1} \text{ s}^{-1}$		51 ± 1	

limiting ($[\text{AcOH}]_{\text{bulk}} \rightarrow 0$) slopes of the plots of k_{decay} vs bulk AcOH concentration for the three derivatives are given in Table 1.

Addition of MeOH or AcOH to MeCN solutions of **4** and **5** had effects similar to those in hexane solution; the lifetimes of the germene absorptions at 325 nm were shortened and the intensities of the underlying long-lived absorptions were reduced as the concentration of added substrate was increased. As in the experiments in hexane solution, pseudo-first-order rate constants for decay of the major (germene) component were determined by nonlinear least-squares fitting of the data to the sum of two exponential decays. Plots of k_{decay} vs $[\text{MeOH}]$ again exhibited strong positive curvature but fit acceptably to the quadratic dependence on $[\text{MeOH}]$ of eq 13. The data are shown in Figure 5b along with corresponding data for quenching of germene **1** by the alcohol, which are in excellent agreement with our earlier published data.¹⁷ The analyses afforded second-order rate coefficients indistinguishable from zero within experimental error in each case, indicative of a pure squared dependence of the rate on alcohol concentration. The effective third-order rate coefficients were thus obtained by linear least-squares analysis of plots of k_{decay} vs $[\text{MeOH}]$,² which showed excellent linearity, and are given in Table 2 for the three compounds. We also examined the quenching of germenes **6** and **7** by MeOD in MeCN, and again the k_{decay} values varied linearly with the square of the alcohol concentration. Analysis

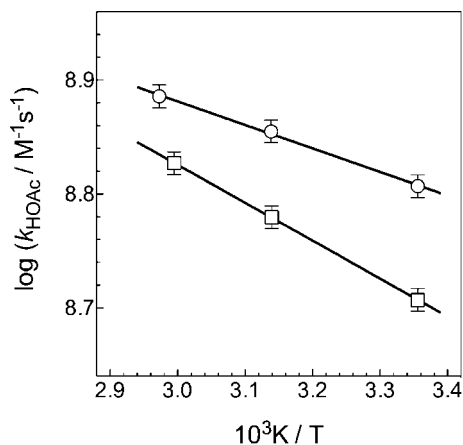


Figure 6. Arrhenius plots for the reaction of germenes (O) **1** and (□) **6** with AcOH in MeCN solution.

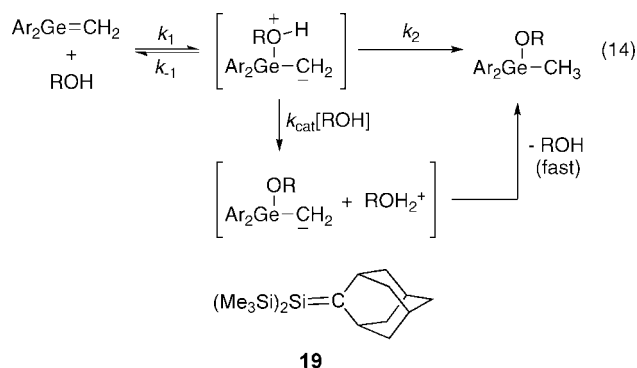
of the data afforded values of $k_{2\text{MeOD}}$ that were in both cases consistently smaller than the corresponding values for the protiated substrate (see Table 2). Finally, quenching of germene **7** by MeOH was also studied in THF solution. The resulting nonlinear plot of k_{decay} vs $[\text{MeOH}]$ was analyzed according to eq 13, with k_0 constrained to a non-negative value. This afforded the second- and third-order rate coefficients $k_{\text{MeOH}} = (2.6 \pm 0.9) \times 10^6 \text{ M}^{-1} \text{ s}^{-1}$ and $k_{2\text{MeOH}} = (3.3 \pm 0.3) \times 10^7 \text{ M}^{-2} \text{ s}^{-1}$, respectively, where the errors are quoted as twice the standard deviation from nonlinear least-squares analysis of the data. Linear plots of k_{decay} vs $[\text{AcOH}]$ were obtained in quenching experiments with the carboxylic acid in MeCN and so were analyzed according to eq 12; the results of these analyses are also given in Table 2. We also redetermined the rate constant for reaction of germene **1** by AcOH in this solvent and obtained a value of $k_{\text{AcOH}} = (6.4 \pm 0.4) \times 10^8 \text{ M}^{-1} \text{ s}^{-1}$, in reasonable agreement with the value reported in our earlier study.¹⁷ Quenching of germene **6** by AcOD in dry MeCN was also investigated, and the experiment afforded a rate constant identical with that obtained with AcOH within experimental error. Finally, quenching of germenes **1** and **6** by AcOH was also studied at 45 and 60 °C, leading to values of k_{AcOH} that increased modestly with increasing temperature in both cases (see Figure S12 in the Supporting Information). The resulting (three-point) Arrhenius plots showed excellent linearity (see Figure 6) and afforded the Arrhenius parameters given in Table 3. For comparison, the published Arrhenius parameters for reaction of the homologous 1,1-diarylsilene derivatives with AcOH in the same solvent³² are also given in Table 3.

The lifetimes of **6** and **7** in hexane solution were also found to be reduced significantly upon addition of acetone (0.05–0.15 M) or *n*-butylamine (*n*-BuNH₂; 1–25 mM). Plots of k_{decay} vs $[\text{Q}]$ according to eq 12 were linear in all cases, except for germene **7** with *n*-BuNH₂, which exhibited a mild positive curvature (see Figure S14 in the Supporting Information). Table 1 contains the rate coefficients obtained from analysis of the data according to eqs 12 and 13, along with our previously reported value for quenching of germene **1** by *n*-BuNH₂ in hexane.¹⁸ Linear plots of k_{decay} vs $[\text{Q}]$ were also obtained for quenching of **6** and **7** by acetone-*d*₆ and afforded k_{Q} values of $(5.0 \pm 0.3) \times 10^5 \text{ M}^{-1} \text{ s}^{-1}$ ($k_{\text{H}}/k_{\text{D}} = 1.62$) and $(6.8 \pm 0.3) \times 10^5 \text{ M}^{-1} \text{ s}^{-1}$ ($k_{\text{H}}/k_{\text{D}} = 2.38$), respectively.

Discussion

The kinetic results for quenching of the three 1,1-diarylgermenes by MeOH and *t*-BuOH in hexane (see Table 1) and by MeOH in MeCN (see Table 2) indicate that the dominant reaction pathway for addition of the alcohols to all three compounds involves two molecules of alcohol in the rate-determining step for the reaction. The overall third-order rate constants increase only very modestly with increasing electron-withdrawing power of the aryl substituents; a three-point Hammett plot of the data for MeOH in MeCN affords a reaction constant of $\rho = +0.19 \pm 0.07$. The reactions in MeCN are subject to small but clearly primary deuterium kinetic isotope effects with both **6** ($k_{\text{H}}/k_{\text{D}} = 1.39 \pm 0.07$) and **7** ($k_{\text{H}}/k_{\text{D}} = 1.5 \pm 0.1$), indicating that proton transfer occurs in the rate-controlling step.

One possible mechanism that is compatible with these results is a two-step process involving reversible reaction of the germene with a single molecule of the alcohol in the initial step, to form a zwitterionic intermediate (or association complex) that proceeds to product by rate-controlling transfer of the proton from the hydroxylic oxygen to the germenic carbon in the second step, either by unimolecular means (resulting in overall second-order kinetics) or by a catalyzed pathway involving the second alcohol molecule as the catalyst (resulting in overall third-order kinetics). The mechanism is shown in eq 14. The two proton-transfer pathways normally compete with one another in the addition of alcohols to transient silenes, though they may not both be detectable in time-resolved experiments.⁹ With particularly electrophilic silenes (such as **3**) only the unimolecular H-transfer pathway is resolvable in kinetic experiments carried out on the microsecond time scale, because it is so fast that one loses the ability to detect the silene at all at the higher concentrations necessary for the catalyzed pathway to become competitive; nevertheless, competition kinetics studies have verified that the overall third-order pathway *does* compete with the second-order path at high alcohol concentrations in the addition of MeOH to **3**.²⁰ The third-order pathway becomes increasingly dominant as the electrophilicity of the Si=C bond is reduced through appropriate substitution and is the only detectable mode of reaction in the case of the very weakly electrophilic silene 1,1-bis(trimethylsilyl)-2-adamantylidenesilane (**19**).¹⁵ In this case, however, experimental and theoretical evidence suggests that the reaction in hexane solution occurs concertedly, via reaction with the hydrogen-bonded dimer of the alcohol.¹⁵



In principle, the catalyzed proton-transfer pathway could proceed by sequential deprotonation–protonation or protonation–deprotonation pathways or by a concerted process in which the two events occur simultaneously. In the case of **1**, we proposed earlier that the deprotonation–protonation sequence is most

Table 3. Arrhenius Parameters for the Reactions of Homologous 1,1-Diarylsilenes and 1,1-Diarylgermenes with AcOH in MeCN Solution

metallene	$k_{\text{AcOH}}/10^7 \text{ M}^{-1} \text{ s}^{-1}{}^a$	E_a (kcal mol ⁻¹)	$\log(A/\text{M}^{-1}\text{s}^{-1})$	ΔS^\ddagger (eu)
Ph ₂ Ge=CH ₂ (1)	64 ± 4	0.96 ± 0.09	9.5 ± 0.1	-17.2 ± 0.2
(4-CF ₃ C ₆ H ₄) ₂ Ge=CH ₂ (6)	51 ± 2	1.52 ± 0.05	9.8 ± 0.1	-15.7 ± 0.2
Ph ₂ Si=CH ₂ (3) ^b	130 ± 30	1.9 ± 0.3	10.5 ± 0.4	-12.5 ± 0.9
(4-CF ₃ C ₆ H ₄) ₂ Si=CH ₂ (20) ^b	220 ± 20	3.6 ± 0.5	12.0 ± 0.4	-6 ± 2

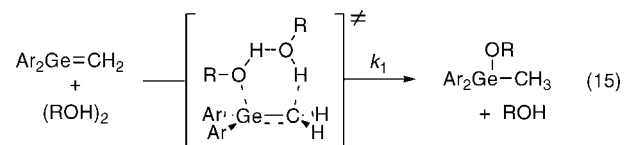
^a At 25 °C. ^b From ref 32.

likely to be correct, on the basis of the observation that the pseudo-first-order decay of **1** in the presence of MeOH and *t*-BuOH in THF solution appeared to exhibit a mixed first- and second-order dependence on alcohol concentration, in contrast to the situation in MeCN, where only the second-order dependence is observed;¹⁷ the (pseudo) first-order component can be interpreted as being due to intervention of the solvent as a catalyst for deprotonation of the complex. The present results for quenching of germene **7** (from **5**) by MeOH in THF confirm this behavior at a level of significance higher than we were able to obtain in the earlier study. In this case, fitting of the k_{decay} vs [MeOH] data to eq 13 (with the constraint $k_0 \geq 0$) leads to second- and third-order rate coefficients of $k_{\text{MeOH}} = (2.6 \pm 0.9) \times 10^6 \text{ M}^{-1} \text{ s}^{-1}$ and $k_{2\text{MeOH}} = (3.3 \pm 0.3) \times 10^7 \text{ M}^{-2} \text{ s}^{-1}$, respectively. While the third-order rate constant is only marginally smaller than that obtained in MeCN solution, the second-order component is of significant magnitude, consistent with the presence of the solvent-catalyzed component of the reaction. Correction of the second-order rate coefficient for the solvent concentration affords an estimate of $k \approx 2 \times 10^5 \text{ M}^{-2} \text{ s}^{-1}$ for the overall third-order rate constant for the solvent-catalyzed reaction pathway, which is ca. 150 times smaller than that for the MeOH-catalyzed pathway. This difference, which should reflect the difference in rate constants for deprotonation of the germene–MeOH complex by THF (in THF) and MeOH (in MeCN), is broadly consistent with the difference in the $\text{p}K_a$ values of protonated THF ($\text{p}K_a$ 1.1) and MeOH_2^+ ($\text{p}K_a$ 2.36) in MeCN solution.³³

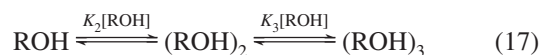
Within the limits of the equilibrium approximation, the observed Hammett ρ value for a two-step reaction mechanism involving a reversibly formed intermediate is equal to the sum of the ρ values for the individual steps in the sequence. Thus, the fact that $\rho_{\text{overall}} \approx 0.2$ indicates that the electronic requirements of the individual steps either oppose one another and almost cancel or that they both are accelerated in a very minor way by electron-accepting substituents on the aryl rings.

A second mechanistic possibility that needs to be considered is a concerted process in which the alcohol reacts with the Ge=C bond via its hydrogen-bonded dimer (eq 15). The involvement of hydrogen-bonded oligomers has been proposed or considered previously in mechanistic studies of a variety of alcohol insertion or addition reactions, including those with singlet carbenes,^{34–38} carbocations,^{38,39} isocyanates,^{40,41} and silenes.¹⁵ The kinetic data

for addition of MeOH to **1**, **6**, and **7** in hexane solution can be analyzed taking this explicitly into account, since equilibrium constants for H-bonded dimer and higher oligomer formation have been reported for MeOH in hexane solution.⁴² Equation 16 defines the mechanistic rate constant in this case, where $[(\text{MeOH})_2]$ is the molar concentration of alcohol dimers in equilibrium with the monomer and higher order oligomers (eq 17). Indeed, plots of k_{decay} vs $[(\text{MeOH})_2]$, the latter calculated from the bulk concentrations using association constants extrapolated from the data of Landeck et al.⁴² ($K_2 = 36.1$, $K_3 = 91.2$ at 25 °C), exhibit good linearity in all three cases (see Figure S11 in the Supporting Information) and afford bimolecular rate constants of $(2.4 \pm 0.2) \times 10^9 \text{ M}^{-1} \text{ s}^{-1}$ for **1**, $(5.5 \pm 0.1) \times 10^9 \text{ M}^{-1} \text{ s}^{-1}$ for **6**, and $(7.2 \pm 0.3) \times 10^9 \text{ M}^{-1} \text{ s}^{-1}$ for **7**. A three-point Hammett plot of these data affords $\rho = +0.26 \pm 0.05$, the same within experimental error as that obtained for the third-order rate constants for reaction of MeOH with the three germenes in MeCN solution (vide supra).



$$k_{\text{decay}} = k_0 + k_1[(\text{MeOH})_2] \quad (16)$$



The self-association of alcohols is of course considerably less favorable in polar, Lewis basic solvents such as MeCN and THF. Nevertheless, Griller, Liu, and Scaiano proposed that the reactions of chlorophenylcarbene with MeOH and *t*-BuOH proceed via the hydrogen-bonded dimers in both isooctane and MeCN, to explain nonlinear kinetic plots similar (in the case of MeOH) to those found in the present work for the three diarylgermenes.³⁴ Kirmse et al. later considered the same mechanism in their study of the reactions of alcohols with siloxycarbenes in MeCN but suggested it was unlikely, citing the fact that they could find no evidence for the presence of H-bonded oligomers of MeOH in MeCN by infrared spectroscopy at concentrations up to 0.4 M.³⁸ On the other hand, the mechanism has received support from recent theoretical calculations,³⁵ and a recent mass spectrometric study of self-association in solutions of MeOH in MeCN shows clear evidence for the presence of both hydrogen-bonded dimers and trimers in significant concentrations at a bulk MeOH concentration of 10 vol % (ca. 0.75 M).⁴³ Unfortunately, none of these studies allow a reasonable estimate to be made for the monomer–dimer

(33) Izutsu, K. *Acid-Base Dissociation Constants in Dipolar Aprotic Solvents*; Blackwell Scientific Publications: Oxford, U.K., 1990; IUPAC Chemical Data Series 35.

(34) Griller, D.; Liu, M. T. H.; Scaiano, J. C. *J. Am. Chem. Soc.* **1982**, *104*, 5549.

(35) Pliego, J. R., Jr.; De Almeida, W. B. *J. Phys. Chem. A* **1999**, *103*, 3904.

(36) Moss, R. A.; Shen, S.; Hadel, L. M.; Kmicik-Lawrynowicz, G.; Wlostowska, J.; Krogh-Jespersen, K. *J. Am. Chem. Soc.* **1987**, *109*, 4341.

(37) Du, X. M.; Fan, H.; Goodman, J. L.; Kesselmayr, M. A.; Krogh-Jespersen, K.; LaVilla, J. A.; Moss, R. A.; Shen, S.; Sheridan, R. S. *J. Am. Chem. Soc.* **1990**, *112*, 1920.

(38) Kirmse, W.; Guth, M.; Steenzen, S. *J. Am. Chem. Soc.* **1996**, *118*, 10838.

(39) Sujdak, R. J.; Jones, R. L.; Dorfman, L. M. *J. Am. Chem. Soc.* **1976**, *98*, 4875.

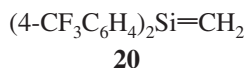
(40) Raspoet, G.; Nguyen, M. T.; McGarraghy, M.; Hegarty, A. F. *J. Org. Chem.* **1998**, *63*, 6867.

(41) Raspoet, G.; Nguyen, M. T.; McGarraghy, M.; Hegarty, A. F. *J. Org. Chem.* **1998**, *63*, 6878.

(42) Landeck, H.; Wolff, H.; Goetz, R. *J. Phys. Chem.* **1977**, *81*, 718.

(43) Rastrelli, F.; Saielli, G.; Bagno, A.; Wakisaka, A. *J. Phys. Chem. B* **2004**, *108*, 3479.

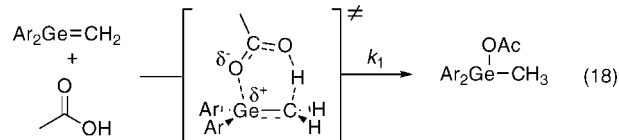
equilibrium constant for MeOH in MeCN at ambient temperatures. We can only note that an observed third-order reaction rate constant ($k_{2\text{MeOH}}$) in the range of $(3-5) \times 10^7 \text{ M}^{-2} \text{ s}^{-1}$ would be consistent with a rate constant (k_1 in eq 16) of a magnitude similar to those estimated in hexane for reaction of the three germenes with MeOH dimers, if the monomer–dimer equilibrium constant is on the order of $K_2 \approx 10^{-2} \text{ M}^{-1}$.⁴⁴ This value actually seems quite reasonable and is consistent with the infrared result of Kirmse et al.,³⁸ given the uncertainties associated with the detection method. The mechanism, if correct, provides a rational explanation for the small primary kinetic isotope effect, the very modest substituent effects on the rates in the two solvents, and the 100-fold rate retardation in MeCN compared to hexane solution, which is then consistent with only a very small solvent effect on the rate constant for the process. A change from a stepwise addition mechanism in the case of 1,1-diarylsilenes to a concerted one in the corresponding germene derivatives seems reasonable, considering the much lower Lewis acidity of the germenes, as evidenced by the fact that silene **3** and the *p*-trifluoromethyl analogue **20** both form detectable solvent complexes in THF solution¹⁰ while the corresponding germene homologues (**1** and **6**) do not. Concerted reaction with the hydrogen-bonded dimer of the alcohol should always be significantly faster than with the monomeric form for two reasons: the process involves a six- rather than a four-center transition state, and the hydrogen-bonded dimer of the alcohol is known to be simultaneously more nucleophilic and more acidic than the monomer.⁴⁵



Quenching of the three germenes by acetic acid proceeds at significantly faster rates than MeOH addition in both hexane and MeCN solution. In hexane, the quenching plots for **6** and **7** both show downward curvature over the 0.5–1 mM concentration range (see Figure S10 in the Supporting Information), which we interpret as being due to self-association of the carboxylic acid in the hydrocarbon solvent; the cyclic hydrogen-bonded dimer of acetic acid can be expected to be much less reactive than the monomer, since both the nucleophilic site (the carbonyl oxygen, presumably) and the acidic hydrogen are engaged in hydrogen bonding to a second molecule of the acid; we assume the reaction proceeds via formal ene addition, involving attack of the carbonyl oxygen at germanium and transfer of the hydroxylic proton to carbon. We failed to detect the nonlinear dependence of k_{decay} on bulk AcOH concentration in our earlier study of **1**, because a much more limited set of kinetic data were collected, over a bulk AcOH concentration range (1–3.5 mM) higher than that used in the present study; given a monomer–dimer equilibrium constant of $K_2 = 3200 \text{ M}^{-1}$,⁴⁶ the acid exists largely as the dimer, and the variation in residual monomeric acid concentration with bulk concentration is approximately linear, over the 1–3.5 mM bulk concentration range. Analysis of the data for all three germenes, taking the self-association equilibrium into account, affords linear plots in all three cases (see Figure S10 in the Supporting Information). The resulting rate constants for reaction with the monomeric form of the carboxylic acid range from $9.2 \times 10^9 \text{ M}^{-1} \text{ s}^{-1}$ for

1 to $7.9 \times 10^9 \text{ M}^{-1} \text{ s}^{-1}$ for **7**, on the basis of the monomer–dimer equilibrium constant reported by Fujii et al. for acetic acid in hexane at 25 °C ($K_2 = 3200 \pm 500 \text{ M}^{-1}$).⁴⁶

As with MeOH quenching, there is again only a very modest variation in the rate constant with aryl ring substituent. This is also true in MeCN solution, for which the plots of k_{decay} vs [AcOH] are linear and the resulting second-order rate constants (Table 2) are ca. 15 times smaller than the corresponding values in hexane. Interestingly, the rates appear to *decrease* slightly with increasing electron-withdrawing power of the aryl substituents, consistent with a Hammett ρ value of $\rho = -0.12 \pm 0.04$ (in MeCN). This is in contrast with the behavior observed for MeOH addition to the three germenes and is also different from the behavior exhibited by the homologous silene derivatives, whose reactions with AcOH in MeCN proceed at rates similar to those in hexane and are characterized by a small *positive* Hammett ρ value ($\rho = +0.17 \pm 0.02$).³² While these results indicate that polar factors play at best only a very small role in the reactions of both the silenes and the germenes with AcOH, they nevertheless indicate that proton transfer is significantly better developed in the transition state for the rate-determining step for addition of AcOH to the germenes than is the case with the silenes. This is in contrast with the situation with MeOH addition, where the effects of substituents on the rate constants are also very small but give rise to positive Hammett ρ values for both the germenes and the silenes. All in all, the results seem most compatible with a concerted mechanism for reaction of AcOH with the germenes, with transfer of the acidic proton to the germenic carbon better developed in the transition state than Ge–O bond formation (eq 18).



The Arrhenius parameters for reaction of AcOH with the two sets of homologous 1,1-diarylgermenes (**1** and **6**) and -silenes (**3** and **20**; see Table 3) provides a particularly interesting indication of the origins of the differences in the reactivities of the two classes of group 14 metallenes with this substrate. It should first be noted that the activation energy increases consistently, and the entropy of activation becomes increasingly positive, with increasing overall reactivity throughout the series **1** < **6** < **3** < **20**, as reflected in the rate constants for reaction at 25 °C. With both sets of compounds, the activation energy is significantly larger and the entropy of activation more positive for the CF₃-substituted derivative than for the parent compound, by a greater margin in the silenes compared to that in the germenes. Thus, for each pair of compounds, increased electron demand in the M=C bond (i.e., by changing the para substituents from H to CF₃) has the counteracting effects of increasing the activation energy and shifting the entropy of activation to more positive values. With the two germenes, the activation energy difference dominates the rate constant ratio (i.e., $k_{1+\text{AcOH}}/k_{6+\text{AcOH}}$) slightly over the entropy difference, and as a result the CF₃-substituted derivative is less reactive than the parent compound. The opposite is true for the silenes, with the result that CF₃ substitution results in an increase in reactivity relative to the parent compound. It should be noted that, for the two silene derivatives, it has been shown that solvent complexation effects contribute to some extent to the measured activation parameters for reaction with nucleophilic substrates in polar

(44) The estimate is derived using the approximation $k_{2\text{MeOH}} \approx k_1 K_2 ([\text{MeOH}]_{\text{bulk}})^2$, where k_1 is the rate constant for the reaction of germene with the methanol dimer.

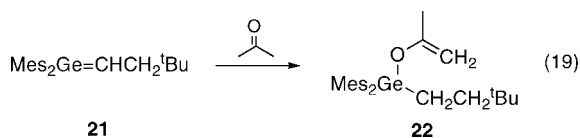
(45) Frange, B.; Abboud, J. L. M.; Benamou, C.; Bellon, L. *J. Org. Chem.* **1982**, *47*, 4553.

(46) Fujii, Y.; Yamada, H.; Mizuta, M. *J. Phys. Chem.* **1988**, *92*, 6768.

solvents,¹⁰ making the differences in both E_a and ΔS^\ddagger between the germenes and silenes, and also between **3** and **20**, appear somewhat larger than they really are. The magnitude of the effect cannot be quantified on the basis of the data available but is presumably not large, since there are no discernible shifts in the UV/vis spectra of **3** and **20** in MeCN relative to hexane solution, even at temperatures as low as 4 °C.¹⁰ It is thus clear that the reaction of AcOH with the silenes is characterized by an extremely loose transition state with minimal Si–O bond formation and O–H bond rupture, with polarity similar to that of the free reactants. In the case of the germenes the reaction proceeds via a lower enthalpic barrier, but through a tighter, relatively nonpolar transition state in which Ge–O bonding and H transfer (in particular) are somewhat better developed than in the case of the silenes. The extent of H transfer must still be relatively small in order to be compatible with the absence of a detectable deuterium kinetic isotope effect.

The reaction of acetone with silenes **3** and **20** also proceeds via formal ene addition, affording the corresponding silyl enol ethers.²³ A two-step mechanism, involving rate-controlling H transfer within a zwitterionic complex, has been proposed on the basis of the marked sensitivity of the rate constant to aryl substituent ($\rho = +1.5$ in isooctane at 25 °C) and isotopic substitution at the ketone α -carbon ($k_H/k_D \approx 2.1$ for **3** in isooctane at 25 °C) and the fact that the reactions of **3** and **20** proceed with negative Arrhenius activation energies.²³ The reaction of silene **20** with acetone proceeds at a rate approaching the diffusion limit in isooctane solution over the -15 to $+10$ °C temperature range.²³

Although we have been unable to obtain evidence for the corresponding reaction products in steady-state photolysis experiments with **2**,¹⁷ **4**, and **5**, the kinetically stable germene 1,1-dimesityl-2-neopentylgermene (**21**) is known to react with this ketone to yield germyl enol ether **22** (eq 19).^{47,48} From this and the fact that lifetime quenching of **6** and **7** by acetone is subject to a distinct primary kinetic isotope effect, we thus conclude that the measured quenching rate constants indeed reflect those for the ene-addition reaction; our failure to detect any actual products of the reaction could be due either to the products being unstable or to the reaction proceeding too slowly to be competitive with other germene-consuming reactions under the conditions of our steady-state photochemical experiments. As mentioned earlier, the reaction of acetone with **1** is too slow to be detected even by flash photolysis, and only an upper limit of roughly $k \approx 10^5 \text{ M}^{-1} \text{ s}^{-1}$ could be established for the rate constant for the putative reaction in the case of the parent compound.¹⁷



The germenes thus react with acetone at least 3 orders of magnitude more slowly than do the homologous silenes under similar conditions, yet they exhibit kinetic isotope effects ($k_H/k_D \approx 1.6$ and 2.4 for **6** and **7**, respectively) that are of magnitudes similar to that exhibited by silene **3** ($k_H/k_D \approx 2.1$)²³ under the same conditions. In spite of this, they appear to exhibit a much smaller substituent effect on the rate; a Hammett ρ value of ca. $+0.3$ is estimated from the difference in rate constants for

quenching of germenes **6** and **7**. The results are again consistent with a significantly less polar transition state for H transfer in the case of the germenes compared to the situation with the corresponding silenes. This is compatible with the results of a recent theoretical study by Mosey et al. of the formal $[2 + 2]$ cycloadditions of formaldehyde with silene and germene, in which it was concluded that the reaction proceeds via a stepwise pathway in both cases, but via a 1,4-zwitterion intermediate in the case of silene and a 1,4-biradical intermediate in the case of germene.⁴⁹

The rate constants for quenching of **1**, **6**, **7**, and 1,1-diphenylsilene (**3**; see Table 1) by *n*-BuNH₂ provide a final point of comparison between the electrophilicities of germenes and silenes of homologous structures. Like alcohols, primary and secondary amines react with **3** by 1,2-addition, again via a stepwise mechanism initiated by nucleophilic attack at silicon followed by rate-controlling proton transfer; the reaction of **3** with *n*-BuNH₂ is the fastest reaction that we have yet encountered with this silene.¹¹ While the course of its reaction with **1** has not been determined, the amine is the one substrate for which it is most reasonable to expect nucleophilic attack at germanium to be the initial step; indeed, the increase in the quenching rate constants throughout the series **1** < **6** < **7** is consistent with this. The fact that the rate constants for amine quenching are of magnitude similar to those for reaction with MeOH, and more than 1 order of magnitude slower than those for reaction with AcOH, is a particularly clear indication of the much reduced electrophilicities of germenes compared to silenes of homologous structure.

Summary and Conclusions

In contrast to 1,1-diarylsilacyclobutanes, whose photolysis in solution affords the corresponding 1,1-diarylsilenes and ethylene as the exclusive products, photolysis of the homologous 1,1-diarylgermacyclobutane derivatives leads to competing (2+2) and (1+3) cycloreversion, affording the corresponding 1,1-diarylgermenes and diarylgermylenes, respectively, along with ethylene and cyclopropane. Germylene formation is enhanced at the expense of germene formation by trifluoromethyl substitution on the aromatic rings and represents the major excited-state decay pathway in the case of 1,1-bis[3,5-bis(trifluoromethyl)phenyl]germacyclobutane (**5**).

The corresponding 1,1-diarylgermenes can be easily detected and studied by laser flash photolysis methods, in spite of minor complications from the germylene coproducts, which are much weaker UV/vis absorbers than the corresponding germenes and hence contribute to the observed transient spectra in only a minor way. The germenes exhibit UV/vis absorption spectra that are similar to one another and to those of the homologous silene derivatives; the absorption maxima are the same in hexane, MeCN, and THF solution and thus do not vary as a function of solvent Lewis basicity. This is indicative of a much weaker Lewis acidity in the cases of the germene derivatives in comparison to that of the homologous silenes, for which the absorption spectra in THF are red-shifted significantly compared to those in hydrocarbon or MeCN solution.¹⁰ The much lower Lewis acidity of germenes compared to silenes is also reflected in the rate constants for quenching of 1,1-diphenylgermene (**1**) and -silene (**3**) by *n*-butylamine; these reactions proceed at close to the diffusion-controlled rate in the case of the silene and

(47) Barrau, J.; Escudie, J.; Satge, J. *Chem. Rev.* **1990**, *90*, 283.

(48) Delpon-Lacaze, G.; Couret, C.; Escudie, J.; Satge, J. *Main Group Met. Chem.* **1993**, *16*, 419.

(49) Mosey, N. J.; Baines, K. M.; Woo, T. K. *J. Am. Chem. Soc.* **2002**, *124*, 13306.

ca. 100 times more slowly than this in the case of the germene. The diarylgermenes studied in this work react much more rapidly with acetic acid than with aliphatic alcohols, which in turn exhibit reactivity significantly higher than that of acetone. In reactions of germenes with substrates of this type, the acidity of the substrate thus has a much greater effect on the reaction kinetics than its nucleophilicity. The opposite is true in the case of the homologous silene derivatives, whose reactions with O- and N-containing substrates characteristically proceed via stepwise mechanisms involving nucleophilic attack at the Si=C bond in the initial step.^{1,9}

Experimental Section

Hexane (BDH Omnisolv), tetrahydrofuran (Caledon Reagent), and diethyl ether (Caledon Reagent) were dried using a Solv-Tek, Inc. solvent drying system. Acetonitrile (HPLC grade) was dried by passage through a column (1 × 6 in.) of neutral alumina, preactivated by heating at 200 °C for 24 h under a stream of dry nitrogen. Methanol, methanol-*O-d*, glacial acetic acid, and acetic acid-*d* were used as received from Sigma-Aldrich Chemical Co. 2,3-Dimethyl-1,3-butadiene and acetone were obtained from Sigma-Aldrich Chemical Co. and were distilled before use. *n*-Butylamine (*n*-BuNH₂; Sigma-Aldrich) was dried by distillation from solid potassium hydroxide. Steady-state photolyses were carried out in a Rayonet photochemical reactor (Southern New England Ultraviolet Co.) equipped with a merry-go-round apparatus and 2–6 RPR-2537 lamps (254 nm). Details of the synthesis and characterization of compounds and photoproducts are described in the Supporting Information.

Nanosecond laser flash photolysis experiments employed the pulses (248 nm; ca. 20 ns; ca. 100 mJ) from a Lambda-Physik Compex 120 excimer laser filled with F₂/Kr/Ne mixtures and a Luzchem Research mLFP-111 laser flash photolysis system, modified as described previously.²⁴ Solutions were prepared at concentrations such that the absorbance at the excitation wavelength was between ca. 0.7 and 0.9 and were flowed continuously through a vacuum-oven-dried, thermostated 7 × 7 mm Suprasil flow cell connected to a calibrated 100 mL reservoir, fitted with a glass frit to allow bubbling of argon gas through the solution. Some experiments were carried out using a simple gravity-flow system, while others employed a Master-

flex™ 77390 peristaltic pump fitted with Teflon tubing (Cole-Parmer Instrument Co.) to pump the solution from the reservoir through the sample cell at more easily controlled rates. The glassware, sample cell, and transfer lines were dried in a vacuum oven at 65–85 °C before use. Solution temperatures were measured with a Teflon-coated copper/constantan thermocouple inserted into the thermostated sample compartment in close proximity to the sample cell. Experiments at temperatures other than 25 °C employed a gravity-flow system and a cell modified to allow insertion of the thermocouple directly into the sample solution. Reagents were added directly to the reservoir by microliter syringe as aliquots of standard solutions. Transient decay and growth rate constants were calculated by nonlinear least-squares analysis of the absorbance–time profiles using the Prism 5.0 software package (GraphPad Software, Inc.) and the appropriate user-defined fitting equations, after importing the raw data from the Luzchem mLFP software. Rate constants were calculated by linear or nonlinear least-squares analysis of decay rate–concentration data (at least seven points; more for data requiring second-order polynomial fitting) that spanned as large a range in transient decay rate as possible. Errors are quoted as twice the standard deviation obtained from the least-squares analyses.

Acknowledgment. We thank the Natural Sciences and Engineering Research Council (NSERC) of Canada for financial support, Teck-Cominco Metals Ltd. for a generous gift of germanium tetrachloride, the McMaster Regional Centre for Mass Spectrometry for high resolution mass spectra, Dr. S. Kornic for elemental analyses, and Dr. C. R. Harrington for the synthesis of **14c**. L.A.H. thanks the NSERC for a graduate scholarship.

Supporting Information Available: Text and figures giving details of the synthesis and characterization of compounds, representative transient decay and growth/decay profiles, time-resolved UV/vis absorption spectra, and details of kinetic analyses. This material is available free of charge via the Internet at <http://pubs.acs.org>.

OM800574S